Theoretical and Experimental Investigation into the Adhesion between Fiber-Reinforced Bitumen and Aggregates by Using Pull-out Method

Mehrdad Masoumi, Sayyed Mahdi Hejazi, and Zeinab Behrouzi

***Abstract*— Using fibers to reinforce bitumen is relatively a new method to improve mechanical properties of asphalt-concrete (AC). Economical competitive advantages, ease of use and improvement of physical and mechanical properties are the benefits of reinforcing AC with fibers in comparison with other modifiers, e.g. polymers. This paper investigates the adhesion of aggregates to fiber-reinforced bitumen. This concept has been described in two parts including theoretical and experimental sections. In the former section, pull-out force of aggregate through fiber-reinforced bitumen has been modeled by using "force-equilibrium method" and "slippage theory of short fiber composites". Therefore, the adhesion force between aggregate and fiber-reinforced bitumen was obtained based on fiber parameters. In the later section, polypropylene (PP) and polyester (PET) fibers of 12 mm length, at fiber content of 0.1%, 0.2% and 0.4% were used to reinforce bitumen. Both of lime and quartz aggregates were considered in the experimental design. Consequently, the Instron tensile tester was modified to perform pull-out tests. Pull-out test measured the force required to pull-out the aggregate through the bitumen and/or fiber-reinforced bitumen. The experimental results showed that the proposed model could predict the pull-out force of fiber-reinforced bitumen samples.**

Keywords: **asphalt concrete, bitumen, fiber, pull-out method, reinforcement**

I. Introduction

Fiber reinforcement of asphalt-concrete (AC) has been very popular and a common method to increase the strength and cracking resistance of the pavement [1]. In fact, inclusion of fibers in paving materials serves to reinforce the pavement by adding additional tensile strength to the material, which results from interconnection between aggregates. This phenomenon may allow the material to withstand additional strain energy before cracking and/or fracture occurs [2]. Over the years, researchers have used different types of fibers to reinforce pavements including polypropylene [1], asbestos [3], glass [2,4], polyester [3], cellulose fibers [3], carbon [3], Kevlar [3], recycled waste fibers [5], and basalt [6]. Moreover, hybrid fiber-reinforcement of AC has recently evolved to include a blend of different fibers to achieve different performance aspects [7,8]. However, a comprehensive literature review shows that polypropylene, polyester and cellulous are the most prevalent fibers used in fiber-reinforced AC mixtures [9]. In brief, Hejazi *et al.* (2011) reported that inclusion of fibers mainly increased dynamic modulus, creep compliance, rutting resistance, moisture susceptibility and freeze-thaw resistance of AC structures. They have also reported a reduction in reflection cracking when AC was modified with polyester fibers [3,10]. A Field investigation of using polyester fibers in asphalt concrete mixtures has shown that fibers increase the elastic recoverability, delay the loss of material stability and change the appearance of rupture, which means an improvement in the fatigue resistance of the pavement [11].

Kaloush and Biligiri (2010) performed a laboratory performance test to reinforce AC by using both polypropylene and aramid (Kevlar) fibers. The test results showed an increase in the shear deformation resistance and the residual strength, meanwhile permanent deformation tests indicated that hybrid fiber-reinforced mixtures accumulated less permanent strain and much higher flow numbers compared to the control mixture [12].

Recently, the distribution effect of steel wool fibers has been investigated on the porosity and electrical conductivity of dense AC. It has been found that long and thin fibers produce many clusters and have a poor distribution within the AC mixture [13].

Qiang *et al.* (2013) suggested using the straw fibers synthesized from agriculture wastes and modified with bentonite to reinforce flexible pavements. The researchers concluded that heat resistance, oil absorbency, and shear performance of straw composite fibers were higher than those of cellulose fibers [14].

Quian *et al.* (2014) examined reinforcing effect of polyester and Kevlar fibers on bitumen at low temperatures. It was concluded that fiber pullout strength can actually exceed the fiber strength due to the coating effect of the bitumen on the surface of fibers [15].

On the other hand, pull-out test is a relatively new method to evaluate the asphalt-aggregate bond and stripping potential of AC mixtures [16]. Australian Standard Test method T-238 was firstly set out the procedure for the assessment of initial adhesion between aggregates and cut back binder with and/or without modifiers under wet or dry test conditions [16]. After that, Tech MRT pull-out test was developed based on T238 which evaluates the initial adhesion between aggregate and any type of binder at higher temperatures to simulate field conditions [16]. Moraes *et al.* (2010) proved that pull-out test is repeatable and reproducible. Therefore, they suggested pull-out test as a practical method to measure the

M. Masoumi, S. M. hejazi, and Z. Behrouzi are with the Department of Textile Engineering, Isfahan University of Technology, Isfahan 84156-83111, Iran. Correspondence should be addressed to S. M. Hejazi (e-mail: hejazi110@cc.iut.ac.ir).

bond strength between aggregates and bitumen in dry and saturated stages under very well controlled conditions [17].

As it can be seen, fiber reinforcement of AC is a relatively new method for producing high performance flexible pavement. Therefore, an investigation into the adhesion between aggregates and fiber-reinforced bitumen is necessary to find the durability of fiber-reinforced asphalt-concrete (FRAC) pavement. On the other hand, pull-out test is a repeatable and reproducible method which measures bond strength between aggregate and bitumen under very well controlled conditions. Consequently, the main aim of this paper is to investigate the pull-out behavior of aggregates through fiber-reinforced bitumen.

II. Materials and Methods

A. Sample Preparation

The bitumen used in this study was prepared from Nafte Jey Company, Isfahan, Iran. Some physical and mechanical properties of the bitumen are shown in Table I. Two types of polymeric fibers were used to reinforce bitumen including polypropylene (PP) and poly(ethylene terphetalate) (PET) fibers. The general specifications of PP and PET fibers are presented in Table II. In addition, two types of aggregates, which are known to have different properties, were selected: limestone and quartz.

TABLE I
Some Physical and Mechanical Properties of Bitumen Used in This Study

parameter	standard method	unit	value
ductility	ASTM D113-79	cm	101
penetration	ASTM D5-73	0.1 mm	69
softening point	ASTM D36-76	ºC	50
flash point	ASTM D92	ºC	309
BBR	AASHTO PP42	ºC	-22

TABLE II
Engineering Specifications of Polypropylene (PP) and Polyester (PET) Fibers Used in This Study

characteristic	value		standard
	PP	PET	
denier, grams per denier	3	2.78	ASTM D-1577
length, mm	12	12	-
tensile strength, MPa	400	900	ASTM D-638
tensile modulus, MPa	1700	15000	ASTM D-638
specific gravity, kg m^{-3}	910	1380	ASTM D-792
melting temperature, ºC	163	260	-

The experimental design of the work included fiber type (PP vs. PET), fiber mass content (0.1%, 0.2% and 0.4%) and aggregate type (limestone vs. quartz) as independent variables, and the response variables were pull-out force and adhesive bond energy. The experimental design is illustrated in Table III. The fiber length was selected to be 12 mm [18].

According to the experimental design, to prepare the samples for pull-out test, PP and/or PET fibers were firstly mixed with bitumen. For this purpose, the bitumen was previously heated up to 132 °C. After that, the reinforced and/or neat bitumen was decanted into a steel saucer. The saucer was filled within one centimeter with reinforced and/or neat bitumen. Simultaneously, aggregate specimens were cut into cubes of $4 \times 4 \times 4$ cm^3. After cutting the aggregates, a five-centimeter steel peg was vertically glued to the top of the aggregates by using a rapid cure epoxy resin. Consequently, the aggregates were immersed in the reinforced and/or neat bitumen depending on the desired sample in accordance with the experimental design (see Fig. 1).

TABLE III
Experimental Design of The Work

treatment description	aggregate type	fiber type	fiber content (wt%)
L	limestone	–	–
L-PET/0.1%	limestone	polyester	0.1%
L-PET/0.2%	limestone	polyester	0.2%
L-PET/0.4%	limestone	polyester	0.4%
Q	quartz	–	–
Q-PET/0.1%	quartz	polyester	0.1%
Q-PET/0.2%	quartz	polyester	0.2%
Q-PET/0.4%	quartz	polyester	0.4%
L-PP/0.1%	limestone	polypropylene	0.1%
L-PP/0.2%	limestone	polypropylene	0.2%
L-PP/0.4%	limestone	polypropylene	0.4%
Q-PP/0.1%	quartz	polypropylene	0.1%
Q-PP/0.2%	quartz	polypropylene	0.2%
Q-PP/0.4%	quartz	polypropylene	0.4%

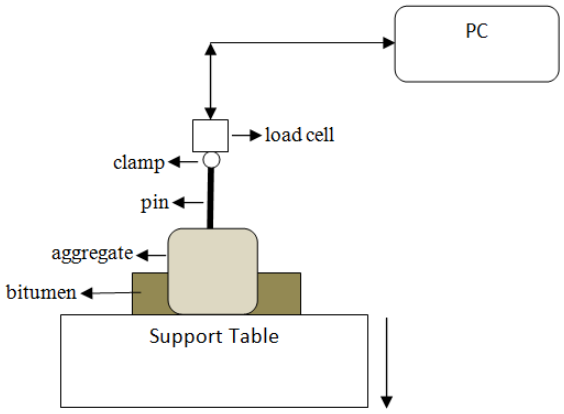

Fig. 1. The pull-out test device provided in this study.

B. Experimental Work

The difficult part of quantitatively evaluating the properties of fiber-bitumen-aggregate systems was to identify the pull-out test. As it was previously indicated, the pull-out test is a simple, quick and repeatable test for evaluating the adhesive bond between modified and/or neat bitumen and aggregates. Consequently, an Instron tensile tester (Zwick universal testing machine 1446 60,1994, Germany) was modified to perform the pull-out test. As illustrated in Fig. 1, the pull-out test device was comprised of a portable lower table, a fixed upper jaw, an LVDT sensor setup on the upper jaw and a digital recorder connected to a PC.

The aggregate surface and pull-out jaws should be degreased with acetone to remove moisture and dust which

could affect the adhesion. To start the test, the steel peg glued to the aggregate was implemented within the upper jaw and the steel saucer containing fiber and/or neat bitumen was screwed to the lower table. Then, the lower table started to move downward to apply a tensile pull-out force on the steel peg, i.e. the aggregate. Therefore, during the test, a pulling force was applied on the specimen. The test speed was selected to be 10 mm min^{-1} [19]. When the applied pull-out stress exceeded the adhesive strength of the binder-aggregate interface the failure occurred or the test was stopped. For each specimen, the pull-out tensile force was continuously measured by the LVDT sensor and transmitted to the PC during the test. Therefore, the PC could draw the force-displacement diagram for each sample. The test was repeated five times for each sample.

The maximum force was extracted from each diagram as the pull-out force. In addition, the pull-out energy and/or the adhesive energy E_d between bitumen and aggregate were calculated for all samples through:

$$E_d = \int_{L=0}^{L=L_{max}} F.dl \quad (1)$$

where L_{max} is the maximum displacement of the aggregate through the bitumen during the pull-out test.

C. Modeling of Adhesion between Aggregate and Fiber-Reinforced Bitumen

As it was previously illustrated the main aim of this paper is to investigate the performance of fibers within bitumen during the pull-out of aggregates through the reinforced binder. Therefore, in this work, "the force equilibrium method" is firstly extended to model the role of fibers in the adhesion improvement of binder-aggregate systems. For simplification, the following assumptions should be considered:

1- According to Fig. 2, the binder is statically settled within the steel saucer with a thickness of *t*.

2- The aggregate P is a cube with dimensions of $a \times a \times a$ cm^3.

3- The aggregate P is vertically immersed into the binder with the wetting thickness of t. Therefore, the aggregate lateral surface S that is involved with the binder will be $4 \times a \times t$.

4- The lower surface of the aggregate P, i.e. $A'B'C'D''$, is in contact with the steel saucer. This assumption fits with the laboratory evidence.

5- The reinforcing fibers have a length of L_f and an elastic modulus of E_f, and are circle in cross-section with a diameter of d_f. The fiber diameter is uniform through the fiber length.

6- The fiber within the bitumen performs linearly elastic during the pull-out test.

Concurrently, as shown in Fig. 3, a fiber identified by the points $DEE'D'$ is considered within the bitumen. It is clear that $\overline{DD'} = L_f$. The fiber makes the orientation angle of γ with the steel saucer and/or the horizon. In addition, the $D'E'$ segment of the fiber is in contact with the aggregate P at the surface $B'BC'C$.

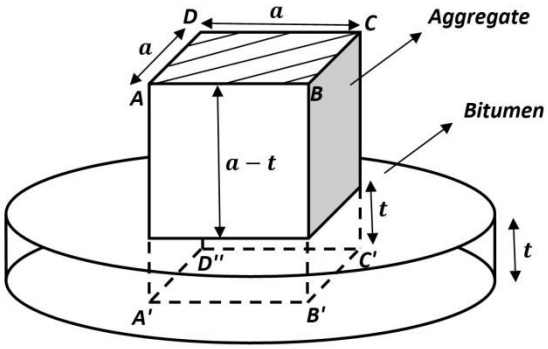

Fig. 2. A schematic drawing of the proposed model.

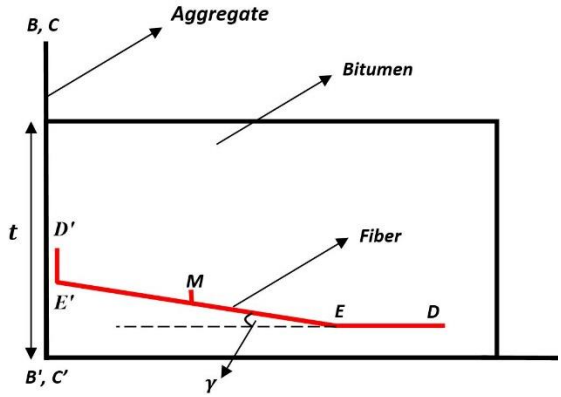

Fig. 3. An aggregate, bitumen and a reinforcing fiber with the initial orientation angle of γ.

At this moment, the aggregate is loaded by a pull-out force of F (see Fig. 4).

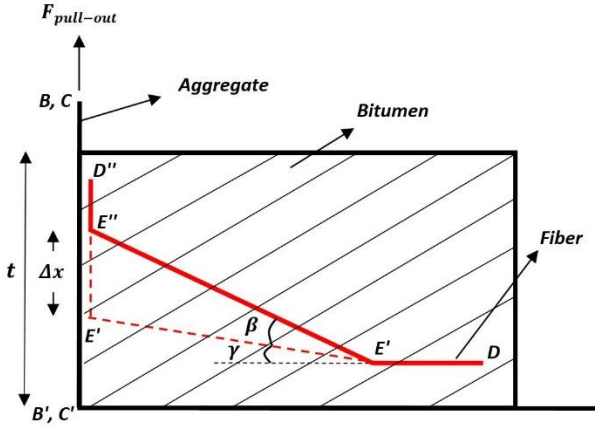

Fig. 4. An aggregate, bitumen and a reinforcing fiber after pull-out loading.

When the aggregate shown in Fig. 4 is displaced a distance of Δx, the fiber segment EE' will be extended within the bitumen matrix to reach EE''.The average tensile stress σ_a within the fiber element depends on the fiber elastic modulus E_f and the strain ε_f induced in the stressed length of the fiber given by:

$$\sigma_a = E_f \times \Delta L_f / L_f \quad (2)$$

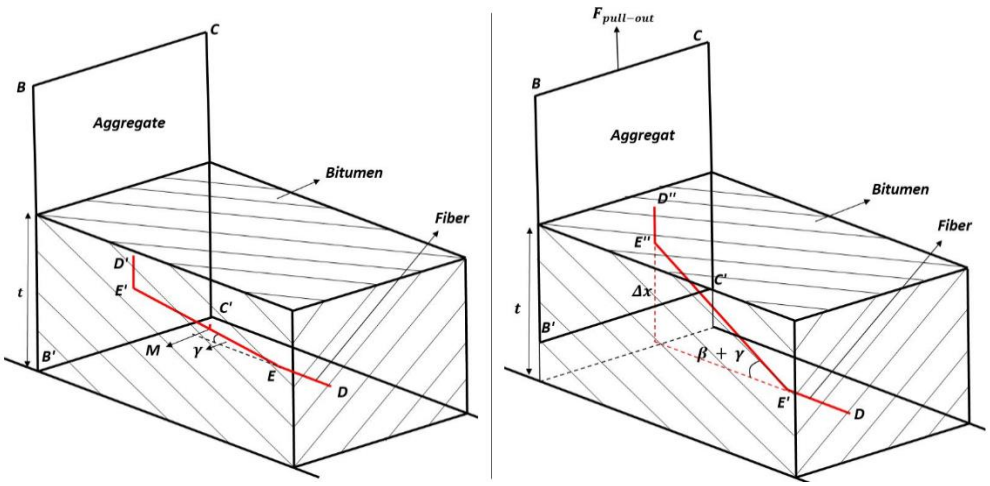

Fig. 5. Comparison of fiber and aggregate positions before (left) and after (right) pull-out loading.

where $\Delta L_f = EE'' - EE'$. Fig. 5 compares the fiber and the aggregate positions before and after pull-out loading for more illustrations.

According to Fig. 4, by considering triangles of EOE', $EE'E''$ and EOE'', one can find the induced strain ε_f as follows:

$$\varepsilon_f = (\cos\gamma/\cos(\gamma+\beta)) - 1 \quad (3)$$

where β is the deformation angle. In Appendix A, it has been proved that β can be obtained through:

$$\beta = \sin^{-1}(\cos\gamma/[\cos^2\gamma + (L_f/\Delta x + \sin\gamma)^2]^{0.5} \quad (4)$$

On the other hand, considering the force equilibrium on a single fiber element, which is shown in Fig. 6, gives the following equation [20, 21]:

$$d\sigma/dL_f = 4\tau/d_f \quad (5)$$

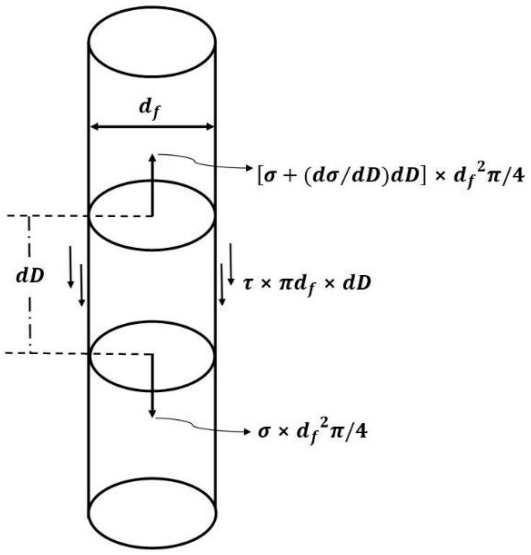

Fig. 6. Force equilibrium within a reinforcing fiber element embedded in a bitumen sample.

Fig. 7 shows the shear and tensile stress distribution within a reinforcing fiber embedded in a bitumen sample by considering the "slippage phenomenon". According to the "slippage theory in short fiber composites" [18], it is supposed that during the extension of a fiber within a matrix, the slippage phenomenon occurs near the both ends of the fiber. Meanwhile there is a central region along the fiber length gripped by the matrix, which is called the non-slippage region.

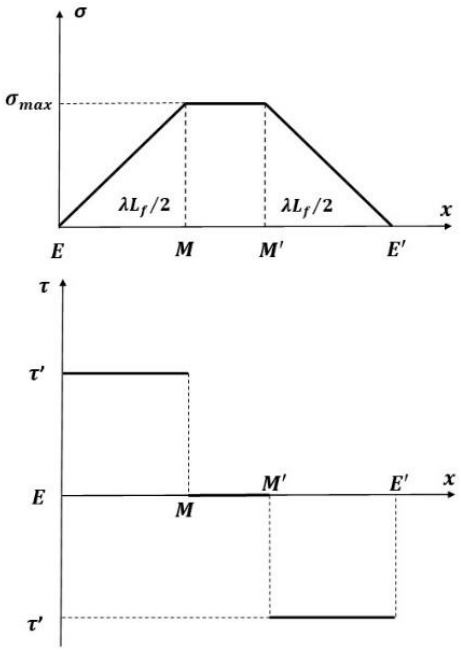

Fig 7. Tensile and shear stress distribution within a reinforcing fiber embedded in a bitumen sample by considering the "slippage phenomenon".

Consequently, the fiber slippage ratio λ is defined as the ratio of fiber length in the slipping region to the whole fiber length L_f. Therefore, the slippage from each end of the fiber will occur over a length of $\lambda L_f/2$ [18, 19]. In other words, λ is an index illustrating the value of fiber cooperation and assistance in the bearing of induced tensile stress during the pull-out loading of the bitumen matrix. If

M is the point on fiber length EE' (see Fig. 7) where the non-slippage region starts and tensile stress rises to the maximum value σ_{max} then integration from Eq. (5) gives the tensile stress σ_{max} at point M:

$$\int_{\sigma=0}^{\sigma=\sigma_{max}} d\sigma = \int_{E}^{M} (4\tau/d_f) dL_f \tag{6}$$

It is noticed that dL_f is equal to dD in Fig. 7. Therefore, σ_{max} will be:

$$\sigma_{max} = (4\tau/d_f) \times \overline{EM} \tag{7}$$

Since $\overline{EM} = \lambda L_f/2$, we have:

$$\sigma_{max} = 2\tau\lambda L_f/d_f \tag{8}$$

On the other hand, according to Fig. 7 the average tensile stress induced within the fiber σ_a could be obtained through:

$$\sigma_{av} = \{ 2\times [\sigma_{max} \times (\lambda \times L_f / 2) / 2] + [(L_f - \lambda \times L_f) \times \sigma_{max}]\} / L_f \tag{9}$$

Consequently, σ_{av} will be:

$$\sigma_{av} = \sigma_{max} \times (1 - \lambda/2) \tag{10}$$

Combination of Eqs. (2), (3) and (10) gives:

$$\sigma_{av} = \left(\Delta L_f / L_f\right) E_f \right) = 2\tau\lambda L_f E_f \left((\cos\gamma / \cos\left(\gamma+\beta\right)) - 1\right) / (\sigma_{max} d_f) \tag{11}$$

Putting Eq. (10) in (11), one can obtain:

$$\sigma_{max} \times \left(1 - \lambda/2\right) = 2\tau\lambda L_f E_f \left((\cos\gamma / \cos\left(\gamma+\beta\right)) - 1\right) / (\sigma_{max} d_f) \tag{12}$$

Therefore, σ_{max} will be:

$$\sigma_{max} = \left(2\tau\lambda E_f L_f / d_f\right)^{0.5} \times \left(\left(\cos\gamma / \cos\left(\gamma+\beta\right)\right) - 1\right)^{0.5} \left(1 - \lambda/2\right)^{-0.5} \tag{13}$$

It is clear that the induced tensile force F_{sf} within the single fiber resisting against pull-out force F_p equals:

$$F_{sf} = \sigma_{max} \times A_f \times \sin(\gamma + \beta) \tag{14}$$

in which $A_f = \pi {d_f}^2/4 =$ fiber cross-section area. Now, consider N_f reinforcing fibers randomly distributed within the bitumen-aggregate system shown in Fig. 4. Each fiber makes the orientation angle of γ_i rwith the horizon. Therefore, according to Eqs. (13) and (14), the total induced tensile force F_f resisting against pull-out force F_p is proportional to:

$$F_f = \pi d_f^2 / 4 \times \sum_{i=1}^{N_f} \left[\left(2\tau\lambda E_f L_f / d_f\right)^{0.5} \times \left(\left(\cos\gamma/\cos(\gamma+\beta)\right) - 1\right)^{0.5} \times (1-\lambda/2)^{-0.5} \times \sin(\gamma_i + \beta_i) \right] \tag{15}$$

where based on Eq. (4), β_i is:

$$\beta_i = \sin^{-1}(\cos\gamma_i / \left[\cos^2\gamma_i + (L_f/\Delta x + \sin\gamma_i)^2\right]^{0.5} \tag{16}$$

In Eq. (15), the number of reinforcing fibers N_f is an unknown that can be calculated through (see Appendix B):

$$N_f = 4 m_b V_f / (\pi {d_f}^2 p_b L_f) \tag{17}$$

where m_b, V_f, and p_b are the bitumen mass, the fiber volume fraction and the bitumen density, respectively.

IV. Results and Discussion

Fig. 8 shows the deformation angle β versus the fiber orientation angle γ based on Eq. (4). It can be seen that the deformation angle β decreases by increasing the fiber orientation angle γ. On the other hand, the more the fiber length, the less the deformation angle β would be, regardless of fiber orientation angle γ. Fig. 8 also states that when the fiber is parallel with the aggregate surface $B'BCC'$, i.e. $\gamma = 90°$, the fiber does not deform during the pull-out loading of the system.

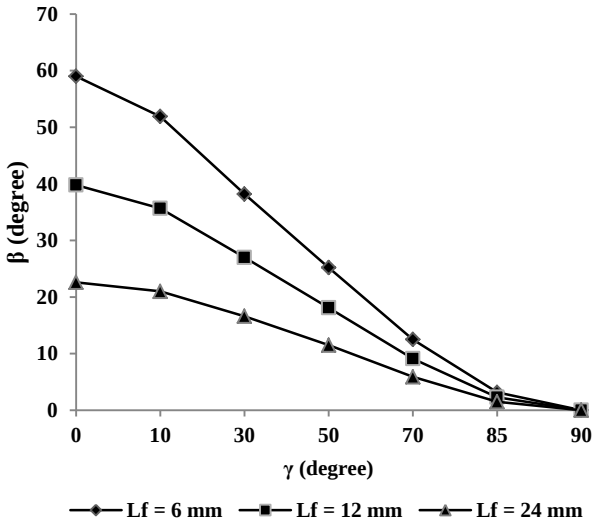

Fig. 8. Deformation angle β versus fiber orientation angle γ at different fiber lengths with $\Delta x = 10$ mm.

According to Eq. (3), the strain induced within the fiber depends on fiber orientation angle γ and deformation angle β as shown in Fig. 9. It is obvious that increasing the fiber orientation angle γ increases the induced strain within the fiber. This is due to the fact that β is decreased as γ increases (see Fig. 8), while ε_f is increased. It is important

to point that an increase in fiber length leads to a decrease in the induced strain within the fiber.

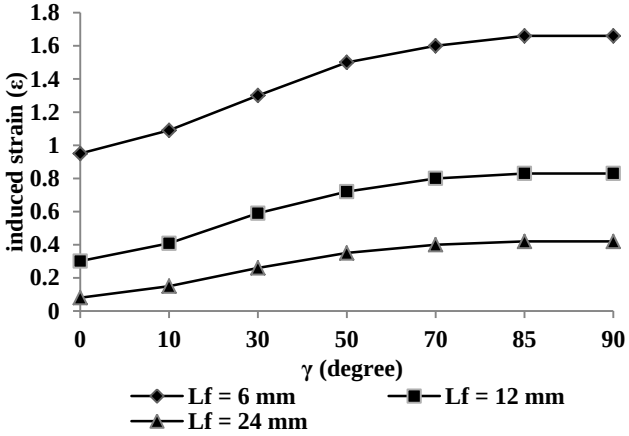

Fig. 9. The effect of fiber orientation angle γ on the strain induced within the fiber at different fiber lengths with $\Delta x = 10$ mm.

Fig. 10 demonstrates the relationship between pull-out force and fiber diameter at various E_f values. The diagram has been drawn by using Eq. (15). It can be concluded that increasing the fiber diameter increases the pull-out force of aggregate through the fiber-reinforced bitumen. This trend will be resonated as the fiber modulus increases from 170 to 170000 MPa at any fiber diameter. It is clear that the more the fiber modulus is, the more the tensile stress will be induced within the deformed fiber during pull-out loading of the system. Consequently, more induced tension force will be obtained as the fiber diameter increases. Here, the authors emphasize that as the fiber diameter increases, the stress transferred from matrix to fiber will be decreased due to more slippage, but the induced tension force resisting against pull-out loading becomes grater.

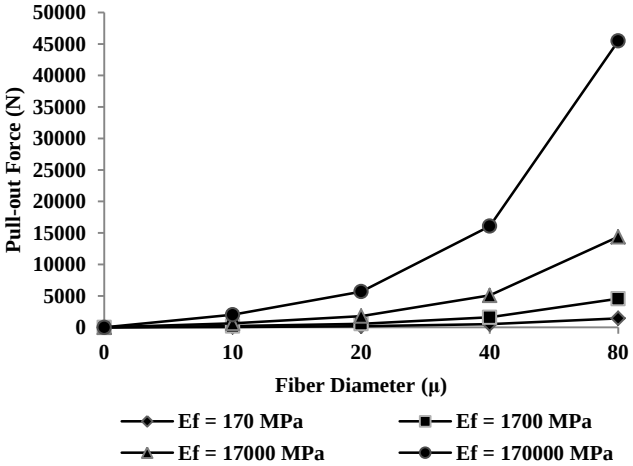

Fig. 10. The relationship between pull-out force and fiber diameter at various fiber moduli:
$\Delta x = 10$ mm, $L_f = 12$ mm, $N_f = 100000$, $\gamma = 45°$ and $\lambda = 0.5$.

Fig. 11 reminds the role of fiber length in pull-out resistance of the system. In the first view, Eq. (15) states that the fiber length L_f directly influences the pull-out force, but a deeper look highlights that as the fiber length increases, the induced tensile strain within the fiber decreases (see Fig. 9).

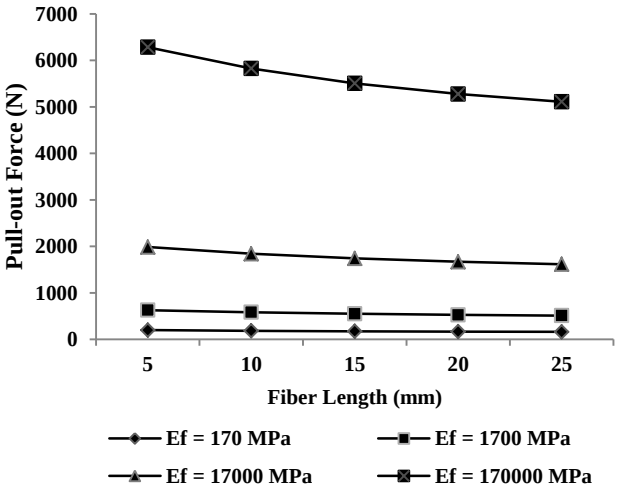

Fig. 11. The role of fiber length in pull-out resistance of the system:
$\Delta x = 10$ mm, $d_f = 20\mu$, $N_f = 100000$, $\gamma = 45°$ and $\lambda = 0.5$.

The relationship between the number of reinforcing fibers N_f and the induced tensile force against pull-out loading is shown in Fig. 12 at various fiber orientation angles (γ). The diagram demonstrates that an increase in both reinforcing fiber numbers N_f and fiber orientation angle γ increases the pull-out force of the system. However, the effect of fiber orientation angle γ is not of such a high degree at lower values of reinforcing fibers N_f, i.e from 10^4 to 2×10^5.

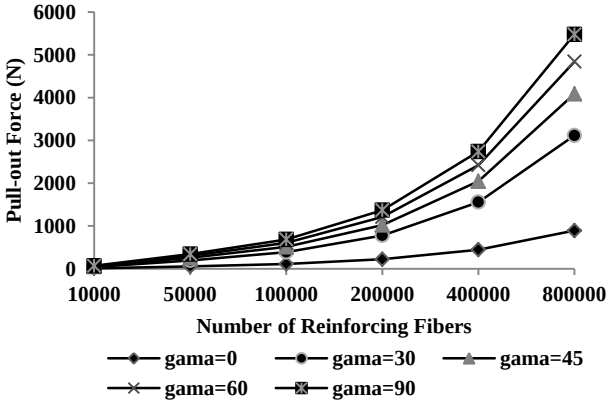

Fig. 12. The relationship between number of reinforcing fibers N_f and induced tensile force against pull-out loading: $\Delta x = 10$ mm, $d_f = 20\mu$, $L_f = 12$ mm and $\lambda = 0.5$.

On the whole, it can be concluded that fiber diameter d_f, fiber length L_f, the adhesion between fiber and bitumen τ, the initial fiber orientation γ, the fiber elastic modulus E_f and the slippage between fiber and bitumen λ determines the induced tensile force within the fiber which is resisting against pull-out loading of the system.

Fig. 13 compares the theoretical results based on proposed model and the experimental data derived from pull-out tests. The theoretical pull-out force of an

aggregate through fiber-reinforced bitumen F_{pt} can be calculated by:

$$F_{pt} = F_s + F_f \tag{18}$$

where F_s is the pull-out force of the aggregate through the neat (unreinforced) bitumen. In this study, F_s was directly obtained by the pull-out tests, and measured 55 and 78 N for limestone and quartz aggregates, respectively. F_f was calculated by using Eq. (15) for each treatment. To facilitate the application of the proposed model, it was assumed that a quarter of reinforcing fibers were oriented around the aggregate with $0 < \gamma < \pi/2$. As it can be seen there is a strong agreement between theoretical results and experimental data. Fig. 13 notes that the pull-out force is directly influenced by fiber content. An increase in fiber content from 0.1% to 0.4% means an increase in the number of reinforcing fibers N_f. However, when the fiber content regardless of fiber type reached 0.4%, the model could not correctly predict the pull-out force of the system (e.g. the treatments of L-PET/0.4, Q-PET/0.4, L-PP/0.4 and Q-PP/0.4). It seems that at higher fiber content (0.4% compared to 0.2%), folding, clumping and balling of fibers decrease the reinforcing performance of fibers. This result is consistent with those obtained by Hejazi *et al.* (2014) in the case of polypropylene fiber reinforced soil composite mixtures [21].

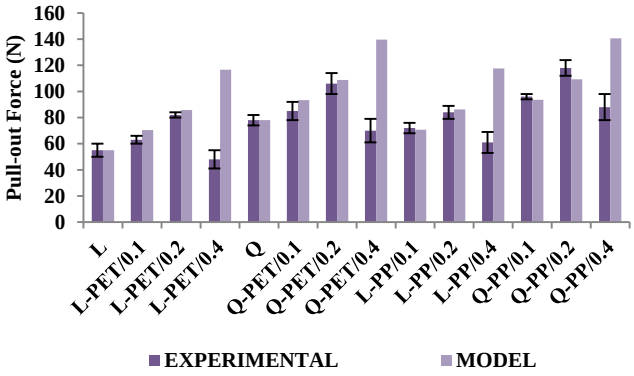

Fig. 13. Comparison of pull-out force values derived from experimental data and model results.

V. Conclusion

This paper investigated the pull-out behavior of an aggregate through fiber reinforced bitumen. The work was established on two parts including experimental and theoretical sections. The experimental design of the work considered the fiber type (PP vs. PET), the fiber mass content (0.1%, 0.2% and 0.4%) and the aggregate types (limestone vs. quartz) as independent variables, while the response variable was the pull-out force. According to the experimental results, the maximum pull-out force was obtained by reinforcing bitumen with 0.2% of PP fibers in the case of quartz aggregates. In the theoretical section, an analytical model was proposed based on the force equilibrium method. The model demonstrated that fiber diameter d_f, fiber length L_f, the adhesion between fiber and bitumen τ, the initial fiber orientation γ, the fiber elastic modulus E_f and the slippage between fiber and bitumen λ determines the induced tensile force within the fiber which is responsible for resisting against pull-out loading of the system. On the whole, there is a strong agreement between theoretical results and experimental data. However, at higher fiber content, the model could not correctly predict the pull-out force of the system. This phenomenon was explained by folding, clumping and balling of the fibers, which decrease the reinforcing performance of the fibers. For future work, it is recommended to use the proposed method and model to investigate the stripping potential of aggregates within neat and/or fiber reinforced bitumen at saturated conditions and different temperatures.

Appendix A: Calculation of Deformation Angle β

For more illustration, the triangles EOE', EOE'' and $EE'E''$ shown in Fig. 6 are extended here:

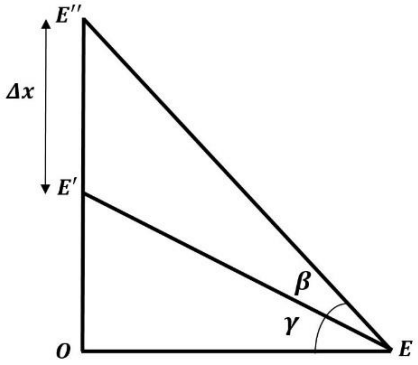

Fig. A1. Fiber deformation (from $EE' = L_f$ *to* EE'') during pull-out test.

It is clear that the induced strain within the fiber ε_f will be:

$$\varepsilon_f = (EE'' - EE')/EE' = (EE''/EE') - 1 \tag{A1}$$

in $\Delta EOE''$:

$$EE'' = (OE' + \Delta x)/\sin(\gamma + \beta) \tag{A2}$$

in $\Delta EOE'$:

$$EE' = OE'/\sin\gamma \tag{A3}$$

in $\Delta EE'E''$:

$$\begin{aligned} L_F \,/\, \sin\left(\pi/2 - \gamma - \beta\right) &= EE'' / \sin(\pi/2 + \gamma) \\ &= \Delta x \,/\, \sin\beta \end{aligned} \tag{A4}$$

Equation (A4) gives:

$$\sin\beta/\cos(\gamma + \beta) = \Delta x/L_F \tag{A5}$$

with being $\cos(\gamma + \beta) = \cos\gamma \times \cos\beta - \sin\gamma \times \sin\beta$, and $\cos\beta = (1 - \sin^2\beta)^{0.5}$, we obtain through Eq. (A5):

$$\sin\beta = \cos\gamma / \left[\cos^2\gamma + (L_f/\Delta x + \sin\gamma)^2\right]^{0.5} \quad \text{(A6)}$$

and therefore:

$$\beta = \sin^{-1}(\cos\gamma / \left[\cos^2\gamma + (L_f/\Delta x + \sin\gamma)^2\right]^{0.5} \quad \text{(A7)}$$

Appendix B: Calculating the Total Number of Reinforcing Fibers within Bitumen

consider a mass of bitumen m_b reinforced with N_f short staple fibers having the length of L_f. The fiber volume fraction v_f is therefore:

$$v_f = V_f/V_b \quad \text{(B1)}$$

where V_f and V_b are the total volume of reinforcing fibers and the volume of the bitumen, respectively. It is clear that:

$$V_f = N_f \times V_{sf} \quad \text{(B2)}$$

and

$$V_b = m_b/p_b \quad \text{(B3)}$$

in which $V_{sf} = \pi {d_f}^2/4 \times L_f$= single fiber volume. Merging Eq. (B1) with Eq. (B3) gives:

$$N_f = 4m_b v_f/(\pi {d_f}^2 p_b L_f) \quad \text{(B4)}$$

REFERENCES

[1] M. Amuchi, S. M. Abtahi, B. Kusha, S. M. Hejazi, and H. Sheikhzeinodin, "Reinforcement of steel-slag asphalt concrete using polypropylene fibers", *J. Ind. Text.*, vol. 44, no.4, pp. 526-541, 2015.

[2] A. Mahrez, M. Karim, and H. Katman, "Fatigue and deformation properties of glass fiber reinforced bituminous mixes", *East Asia Soc. Trans. Stud.*, vol. 6, pp. 997–1007, 2005.

[3] S. M. Abtahi, M. Sheikhzadeh, and S. M. Hejazi, "Fiber-reinforced asphalt-concrete – A review", *Constr. Build. Matter.*, vol. 24, no. 6, pp. 871-877, 2010.

[4] A. Mahrez, M. Karim, and H. Katman, "Prospect of Using Glass Fiber Reinforced Bituminous Mixes", *East Asia Soc. Trans. Stud.*, vol. 5, pp. 784-807, 2003.

[5] B. Putman and S. Amirkhanian, "Utilization of Waste Fibers in Stone Matrix Asphalt Mixtures", *Resour, Conserv. Recy.*, vol. 42, no. 3, pp. 265-274, 2004.

[6] N. Morova, Investigation of usability of basalt fibers in hot mix asphalt concrete, *Constr. Build. Matter*., vol. 47, pp. 175-180, 2013.

[7] F. Corportation, Inc., FORTA-FI® Fiber Reinforcement Technology for Asphalt. www.forta-fi.com

[8] NYCON Inc. Hot Mix Asphalt Applications. Available: www.nycon.com/nycon-fibers-for-asphalt

[9] S. M. Abtahi, M. G. Ebrahimi, M. Kunt, S. M. Hejazi, and S. Esfandiarpour, "Hybrid Reinforcement of Asphalt-Concrete Mixtures Using Glass and Polypropylene Fibers", *J. Eng. Fiber. Fabr.*, [online]. Available: http://www.jeffjournal.org/papers/Volume8/JEFF8-02-03.Hejazi.S.pdf.

[10] D. A. Maurer, "Comparison of methods to retard reflective cracking in bituminous concrete pavements using fabrics and fibers: construction and early performance report", Pennsylvania Dept. of Transportation, Research Project No. 83-8. Available: http://adsabs.harvard.edu/abs/1985STIN...8625522M.

[11] Z. Haoran, Y. Jun, C. Ling, C. Juan, and W. Jun, "Influence of polyester fibre on the performance of asphalt mixes", In: *Proceedings of the 26th Southern African Transport Conference (SATC 2007)*, Pretoria, South Africa, 2007. Available: http://www.repository.up.ac.za/handle/2263/6004.

[12] K. Kaloush, K. Biligiri, W. Zieada, M. Rodezno, and J. Reed, "Evaluation of Fiber-Reinforced Asphalt Mixtures Using Advanced Material Characterization Tests", *J. Test. Eval.*, vol. 38, no. 4, pp. 1-12, 2010.

[13] A. García, J. Norambuena-Contreras, M. N. Partl, and P. Schuetz, "Uniformity and mechanical properties of dense asphalt concrete with steel wool fibers", *Constr. Build. Mater.*, vol. 43, pp. 107-117, 2013.

[14] X. Qiang, L. Lei, and C. Yi-jun, "Study on the action effect of pavement straw composite fiber material in asphalt mixture, Construction and Building Materials", *Constr. Build. Mater.*, vol. 43, pp. 293-299, 2013.

[15] S. Qian, H. Ma, J. Feng, R. Yang, and X. Huang, "Fiber reinforcing effect on asphalt binder under low temperature, Construction and Building Materials", *Constr. Build. Mater.*, vol. 61, pp. 120-124, 2014.

[16] S. K. Das, "Evaluation of asphalt-aggregate bond and stripping potential", *MSc. thesis*, Dept. Civil Eng., Texas Tech University, Texas, USA, 2004. Available: https://ttu-ir.tdl.org/ttu-ir/handle/2346/15840.

[17] R. Moraes, R. Velasquez, and H. Bahia, "Measuring effect of moisture on asphalt-aggregate bond with the bitumen bond strength test", *Transport. Res. Rec.*, vol. 2209, pp. 70-81, 2011.

[18] S. M. Hejazi, M. Abtahi, M. Sheikhzadeh, and D. Semnani, "Introducing two simple models for predicting fiber reinforced asphalt concrete (FRAC) behavior during longitudinal loads", *Int. J. Appl. Polym. Sci.*, vol. 109, no. 5, pp. 2872-2881, 2008.

[19] L. J. Waldron, "Shear resistance of root-permeated homogeneous and stratified soil", *Soil. Sci. Am. J.*, vol. 41, No. 5, pp. 843-849, 1977.

[20] S. M. Hejazi, M. Sheikhzadeh, S. M. A., V. Malekian, and S. Mahmoodi, "Using slippage theory to analyze shear behavior of loop-formed fiber reinforced soil composites"', *J. Ind. Text.*, vol. 43, no. 3, pp. 415–439, 2014.

[21] S. M. Hejazi, A. R. Baghulizadeh, M. Nateghi, and M. Mardani, "Shear modeling of polypropylene-fiber reinforced soil composite using electrical conductivity contour technique", *J. Ind. Text.*, vol. 45, no. 1, pp. 133-151, 2015.